



Contents lists available at ScienceDirect

IJC Heart & Vasculature

journal homepage: www.journals.elsevier.com/ijc-heart-and-vasculature

Diagnostic value of quantitative parameters for myocardial perfusion assessment in patients with suspected coronary artery disease by single- and dual-energy computed tomography myocardial perfusion imaging

Aroa Ruiz-Muñoz^{a,b,c,d}, Filipa Valente^{a,b,c,d}, Lydia Dux-Santoy^{a,b,c,d}, Andrea Guala^{a,b,c,d}, Gisela Teixidó-Turà^{a,b,c,d}, Laura Galián-Gay^{a,b,c,d}, Laura Gutiérrez^{a,b,c,d}, Rubén Fernández-Galera^{a,b,c,d}, Guillem Casas^{a,b,c,d}, Teresa González-Alujas^{a,b,c,d}, Ignacio Ferreira-González^{a,c,d,e}, Arturo Evangelista^{a,b,c,d}, José Rodríguez-Palomares^{a,b,c,d,*}

^a Vall d'Hebron Institut de Recerca (VHIR), Barcelona, Spain

^b CIBER-CV, Instituto de Salud Carlos III, Madrid, Spain

^c Department of Cardiology, Hospital Universitari Vall d'Hebron, Barcelona, Spain

^d Universitat Autònoma de Barcelona, Barcelona, Spain

^e CIBERESP, Instituto de Salud Carlos III, Madrid, Spain

ARTICLE INFO

Article history:

Received 3 December 2020

Received in revised form 9 January 2021

Accepted 14 January 2021

Keywords:

Coronary artery disease

Myocardial ischaemia

CT myocardial perfusion imaging

Transmural perfusion ratio

Dual-energy CT-based iodine imaging

ABSTRACT

Purpose: To compare performance of visual and quantitative analyses for detecting myocardial ischaemia from single- and dual-energy computed tomography (CT) in patients with suspected coronary artery disease (CAD).

Methods: Eighty-four patients with suspected CAD were scheduled for dual-energy cardiac CT at rest (CTA) and pharmacological stress (CTP). Myocardial CT perfusion was analysed visually and using three parameters: mean attenuation density (MA), transmural perfusion ratio (TPR) and myocardial perfusion reserve index (MPRI), on both single-energy CT and CT-based iodine images. Significant CAD was defined in AHA-segments by concomitant myocardial hypoperfusion identified visually or quantitatively (parameter < threshold) and coronary stenosis detected by CTA. Single-photon emission CT and invasive coronary angiography were used as reference. Perfusion-parameter cut-off values were calculated in a randomly-selected subgroup of 30 patients.

Results: The best-performing thresholds for TPR, MPRI and MA were 0.96, 23 and 0.5 for single-energy CT and 0.97, 47 and 0.3 for iodine imaging. For both CT-imaging modalities, TPR yielded the highest area under receiver operating characteristic curve (AUC) (0.99 and 0.97 for single-energy CT and iodine imaging, respectively, in vessel-based analysis) compared to visual analysis, MA and MPRI. Visual interpretation on iodine imaging resulted in higher AUC compared to that on single-energy CT in per-vessel (AUC: 0.93 vs 0.86, respectively) and per-patient (0.94 vs 0.93) analyses.

Conclusion: Transmural perfusion ratio on both CT-imaging modalities is the best-performing parameter for detecting myocardial ischaemia compared to visual method and other perfusion parameters. Visual analysis on CT-based iodine imaging outperforms that on single-energy CT.

© 2021 Published by Elsevier B.V. This is an open access article under the CC BY-NC-ND license (<http://creativecommons.org/licenses/by-nc-nd/4.0/>).

* Corresponding author at: Department of Cardiology, Hospital Universitari Vall d'Hebron, Paseo Vall d'Hebron 119-129, 08035 Barcelona, Spain.

E-mail addresses: aroa.ruiz.munoz@gmail.com (A. Ruiz-Muñoz), filipaxaviervale@gmail.com (F. Valente), lydia.dux@gmail.com (L. Dux-Santoy), andrea.guala@yahoo.com (A. Guala), gteixido@vhebron.net (G. Teixidó-Turà), lauragaligan-gay@gmail.com (L. Galián-Gay), lauraguga@gmail.com (L. Gutiérrez), rubenfdezgalera@gmail.com (R. Fernández-Galera), gcasasmasnou@gmail.com (G. Casas), mtegonzalez@vhebron.net (T. González-Alujas), iferreir@vhebron.net (I. Ferreira-González), arturevangelistamasip@gmail.com (A. Evangelista), jfrodriiguezpalomares@gmail.com (J. Rodríguez-Palomares).

1. Introduction

Coronary artery disease (CAD) management has improved over time; however CAD remains the leading cause of morbidity and mortality in the western world [1]. Computed tomography angiography (CTA) is considered an accurate, non-invasive method for the anatomical evaluation of luminal narrowing in coronary arteries. Nonetheless, in patients with known CAD, the addition of computed tomography (CT) myocardial perfusion imaging may

improve the detection of haemodynamically-significant stenosis [2].

CT myocardial perfusion imaging is usually based on visual interpretation of left ventricular contrast enhancement on both rest and stress-induced CT images (CTA and CTP, respectively). However, a quantitative approach could avoid the limitations of subjective visual estimation [3]. Several parameters such as transmural perfusion ratio (TPR) [3–8], myocardial perfusion reserve index (MPRI) [9] and mean attenuation (MA) have been proposed for the quantitative analysis of myocardial perfusion. Nevertheless, comparative studies indicating which parameter is more accurate are lacking.

CT myocardial perfusion imaging can be performed using dual-energy CT, allowing mapping of iodine distribution in the myocardium that can be used as a quantitative perfusion marker [10]. Nonetheless, the benefits of using CT-based iodine images compared to native CT scans for quantitative assessment of myocardial ischaemia have not been sufficiently studied.

This study aimed (1) to compare and rank the performance of quantitative perfusion parameters and visual analysis in the evaluation of myocardial ischaemia by both single- and dual-energy CTA/CTP images in a cohort of patients with chest pain and (2) to ascertain whether the use of dual-energy CT-based iodine imaging has advantages over analysis with single-energy CT scans in the identification of myocardial ischaemia.

2. Materials and methods

2.1. Population and study design

Eighty-four consecutive patients with chest pain, a prior myocardial perfusion single-photon emission computed tomography study, and referred for invasive coronary angiography (ICA) were enrolled in the study. Exclusion criteria were atrial fibrillation, supraventricular arrhythmias, high-grade atrioventricular block, renal insufficiency (estimated glomerular filtration rate < 30 mL/min), chronic obstructive pulmonary disease, significant aortic stenosis, known CAD, coronary percutaneous or surgical revascularisation and contraindication to iodinated contrast.

Before ICA, patients were scheduled for cardiac CT, including dual-energy CTA (rest acquisition) and CTP (stress-induced acquisition) (Fig. 1). Monochromatic images generated from the dual-energy CT scan were used as a surrogate of single-energy CT studies. Myocardial perfusion was assessed by visual interpretation and using three quantitative parameters (TPR, MPRI, and MA) at per-patient and per-vessel levels. Firstly, parameter cut-off values were calculated from a randomly-selected **test group** of 30 patients. Qualitative and different quantitative analyses were compared in a **validation group** of other 54 patients using SPECT + ICA as reference. The study protocol was approved by the institutional Ethics Committee and all participants provided written informed consent.

2.2. Imaging protocols

2.2.1. SPECT

SPECT studies were carried out according to current recommendations [11], following a single-day stress-rest protocol using a technetium-99 m radiotracer. Treadmill exercise was performed according to the Bruce protocol. Image acquisition was conducted with an Elscint SP4 nuclear gamma camera with a high-resolution collimator and short- and long-axis view images were obtained and analysed by two experts. By consensus, SPECT was considered positive if a perfusion defect was shown in at least two of the three axes or in three consecutive views from the same axis with total or partial reversibility at rest.

2.2.2. CTA/CTP

Patients underwent a rest coronary CT angiography (CTA) followed by a Dipyridamole stress-induced CT study (CTP). For CTA, patients were given sublingual nitroglycerine if systolic blood pressure was > 100 mmHg, and intravenous beta-blockers (Esmolol, 1–3 mg/kg) if heart rate was > 60 bpm. Contrast (Iomeron 400) was administered via a cubital vein, with a flow of 5.5 mL/second and volume between 80 and 100 mL depending on the patient's weight. CTP was acquired once Dipyridamole was injected (0.84 mg/Kg over 6 min [12]) into a cubital vein followed by 80 mL of iodine contrast (Iomeron 400) at 4.0–5.0 mL/second for each of the separate, axial, prospectively ECG-triggered acquisitions [2]. Then, all patients received intravenous Aminophylline (250 mg/10 mL) to reverse the effect of Dipyridamole.

The scans were acquired on a 64-slice CT scanner (Discovery CT 750 High Definition; General Electrics (GE); WI; USA) that includes an x-ray source which can switch energy between 80 and 140 kVp within 0.3–0.5 ms, and is complemented by a gemstone detector with fast primary speed and low afterglow.

The scanning protocol was adapted to individual body mass index (calculated as weight divided by square of height; kg/m²) using Gemstone Spectral Imaging (GSI) presets as previously reported in detail [13]. In brief, tube current ranged from 375 to 640 mA, while GSI mode with fast tube voltage switching between 80 and 140 kVp on adjacent views during a single rotation resulted in a mean tube voltage ranging from 105 to 112 kV. The following scanning parameters were used in addition: axial scan mode with 64 × 0.625 mm, gantry rotation time of 350 ms and temporal resolution of 175 ms.

From the acquired data, conventional polychromatic images corresponding to the 140 kVp tube voltage as well as monochromatic image sets from the GSI data file (50, 60, 70, 80, 90, 100, 120 a 140 keV) were reconstructed using Adaptive Statistical Iterative Reconstruction (ASiR) technology [14]. All these data were transferred to a dedicated workstation (AW VolumeShare5 workstation, General Electrics (GE), WI, USA) to obtain CT-based iodine images and the short-axis views of the left ventricle (LV) (basal, mid-cavity and apical) on both single-energy CT (Hounsfield Units) and iodine images for the posterior analysis of myocardial perfusion.

2.3. Myocardial perfusion assessment

Myocardial perfusion defect was defined as the concurrent presence of two conditions: (1) **hypoperfusion in the myocardium** identified through visual or quantitative analysis (parameter < threshold), and (2) **a corresponding significant coronary stenosis** with > 50% or > 70% reduction in vessel lumen on CTA. Each myocardial segment was assigned to one major epicardial coronary artery - left anterior descending artery (LAD), left circumflex artery (LCX) and right coronary artery (RCA) - in accordance with previous recommendations [15] and coronary dominance.

The hypoperfusion in the myocardium was assessed by both single-energy CT and CT-based iodine studies. The LV on CTA (rest acquisition) and CTP (stress-induced acquisition) was divided into equal thirds perpendicular to the long axis using anatomical landmarks and following the published recommendations [15] (Fig. 2). Then the short-axis images of the LV (basal, mid-cavity and apical section) were divided into myocardial segments according to the 16-AHA segmentation model of the LV [15] and assessed for ischaemia both visually and quantitatively by an experienced observer (Figs. 1 and 2). More details about AHA-segmentation in Appendices A1.

Coronary stenosis was evaluated on CTA based on the 17 coronary segment model according to SCCT recommendations [16].

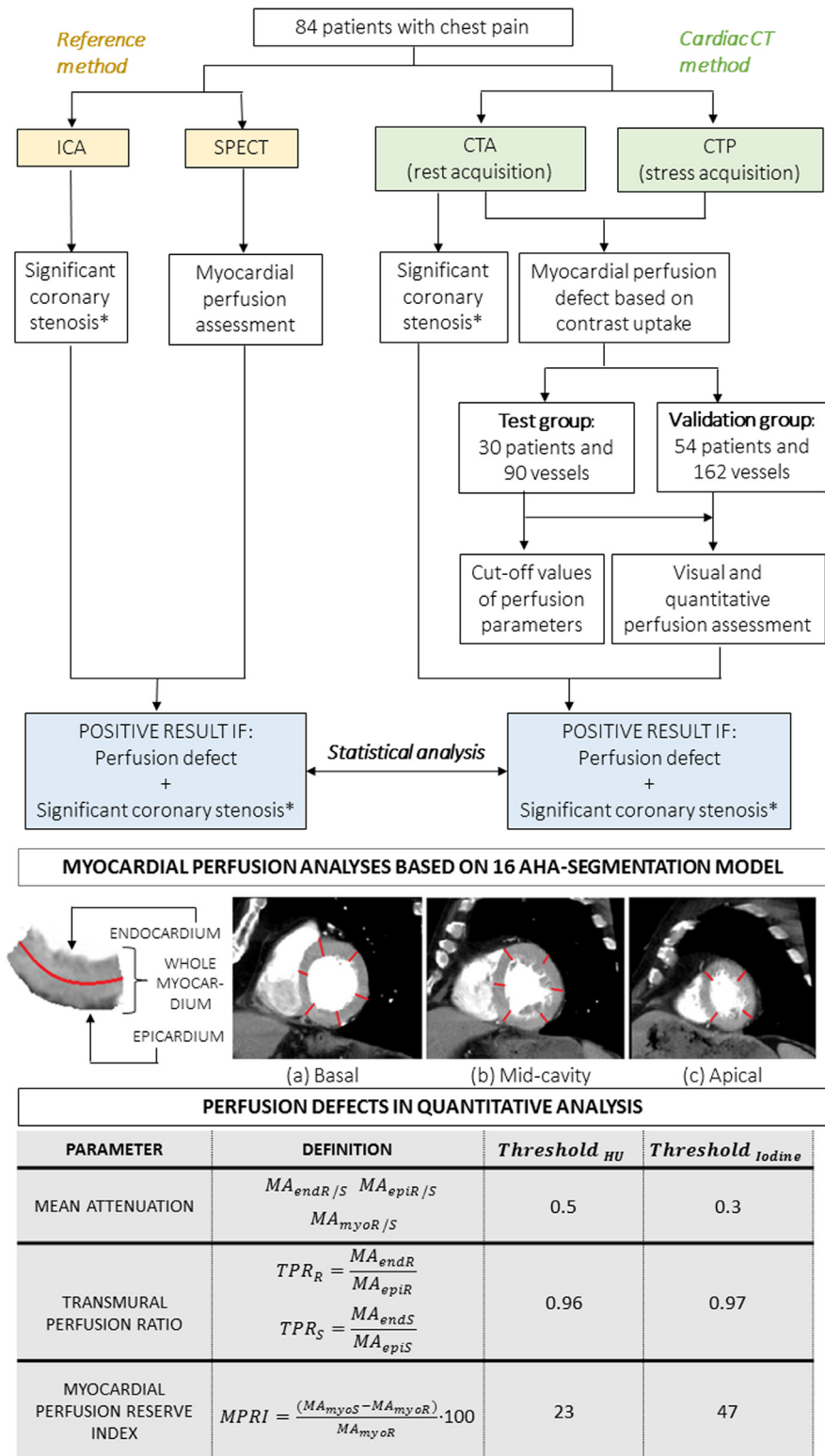


Fig. 1. Algorithm illustrating Computed Tomography (CT) myocardial perfusion analysis.

*Significant coronary stenosis defined with >50% or >70% reduction in vessel lumen on Invasive Coronary Angiography (ICA) or Computed Tomography Angiography (CTA). Abbreviations: AHA = American Heart Association; CTA = Computed Tomography Angiography; CTP = Computed Tomography Myocardial Perfusion study; end = endocardium; epi = epicardium; HU = Hounsfield Units; ICA = Invasive Coronary Angiography; MA = Mean Attenuation; MPRI = Myocardial Perfusion Reserve Index; myo = whole myocardium; R = rest; S = stress; SPECT = Single Photon Emission Computed Tomography; TPR = Transmural Perfusion Ratio.

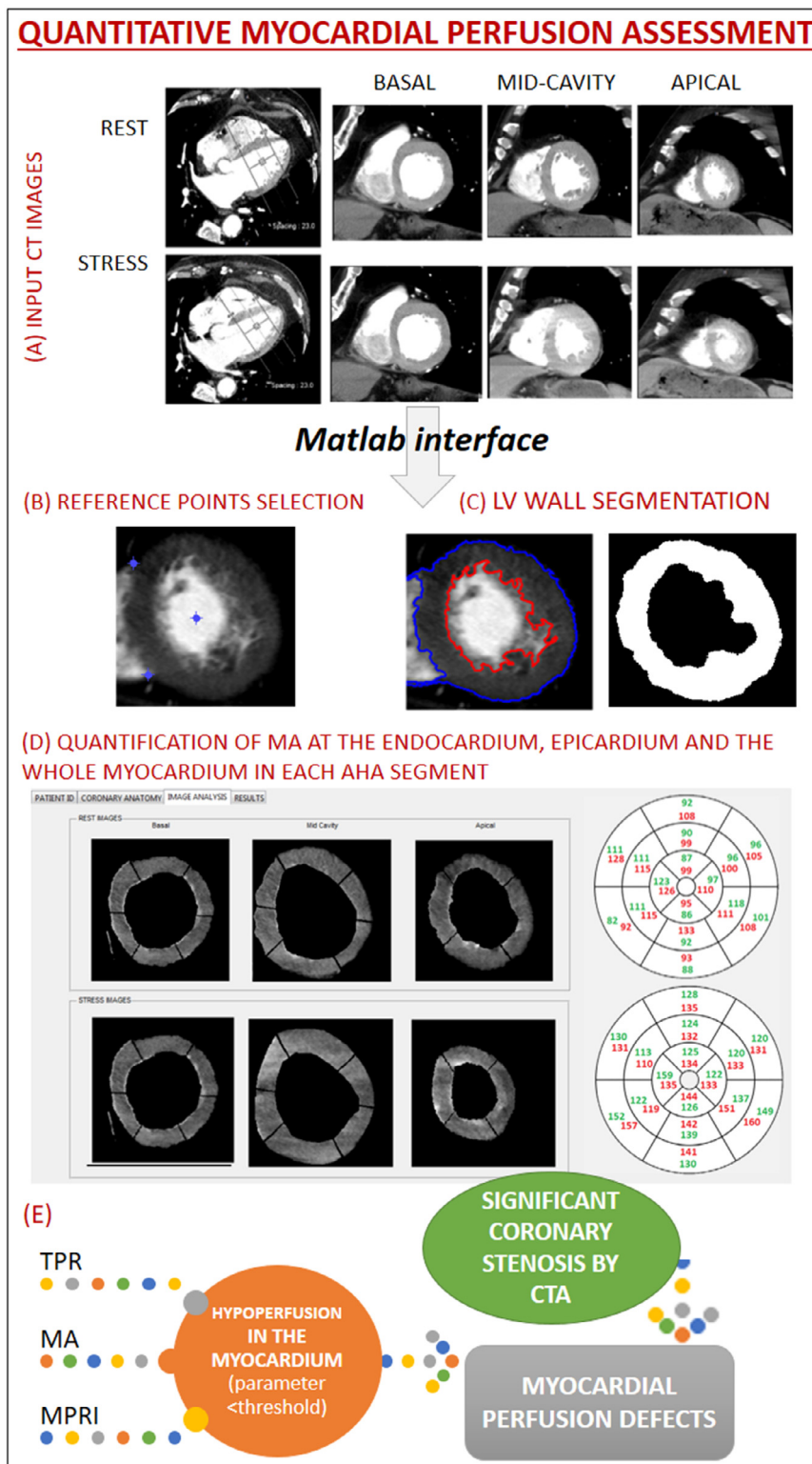


Fig. 2. Quantitative myocardial perfusion analysis. (A) Myocardial perfusion was assessed using three short-axis views of the left ventricle (basal, mid and apical) both at rest and under stress by an experienced observer. (B) For each of the six short-axis views (3 at rest and 3 at stress), three reference points were selected. (C) The left ventricle (LV) wall segmentation was done by Region Growing and using an in-house Matlab code (MathWorks, Massachusetts, US). (D) The mask and reference points were transformed from Cartesian into Polar Coordinate System and the angles of reference points were used to extract myocardial AHA segments. Mean attenuation (MA), transmural perfusion ratio (TPR) and myocardial perfusion reserve index (MPRI) were computed; once attenuation at the subendocardium, subepicardium and the whole myocardium were quantified automatically. (E) Ischaemic perfusion defects were defined as the concurrent presence of two conditions: *myocardial hypoperfusion* identified through quantitative analysis (parameter < reference threshold), and a *corresponding significant coronary stenosis* with > 50% or > 70% reduction in vessel lumen on CTA.

Stenosis was considered significant if coronary vessel diameter was reduced by >50% or >70%, as recommended [2,17].

Diagnostic accuracy of CTA/CTP was evaluated at both per-patient and per-vessel levels with the latter being based on a three-vessel territory model including LAD, LCX and RCA. The performance of CTA/CTP was compared with SPECT + ICA, considered here as a reference. A perfusion defect was defined if SPECT identified hypoperfusion in a region of the myocardium supplied by a stenotic main coronary artery evaluated by ICA (Fig. 1).

2.3.1. Visual assessment

Visual analysis of myocardial perfusion was made in the **validation group**. AHA-segments with hypoperfusion were identified as hypoattenuating (darker) areas containing reduced amounts of contrast material on stress (reversible ischaemia) or on both rest and stress (necrosis) images [3].

2.3.2. Semi-automatic, quantitative assessment

Quantitative myocardial perfusion analysis was made using the following parameters:

- (a) **Mean attenuation (MA)**: mean value of the attenuation of pixels included in the subendocardium (MA_{endR/S}), subepicardium (MA_{epiR/S}), and whole myocardium (MA_{myoR/S}). This parameter was evaluated in both rest (R) and stress (S) images.
- (b) **Transmural perfusion ratio (TPR)**: the MA ratio in the subendocardium relative to the MA of the entire subepicardium of any given short-axis slice [3]. This parameter was evaluated in both rest (R) and stress (S) images.

Table 1
Baseline characteristics.

Characteristic	Test group	Validation group	p-Value
N ₁ Number of subjects	30	54	-
N ₂ Number of vessels	90	162	-
Sex (male)	17 (56.7%)	36 (66.7%)	0.145
Age (years)	71.0 [60.0;74.0]	71 [62.0;74.5]	0.421
Body mass index (kg/m ²)	28.0 [25.0;30.75]	28.0 [26.0;30.0]	0.850
Hypertension	24 (80.0%)	39 (72.2%)	0.124
Diabetes mellitus	12 (40.0%)	17 (31.5%)	0.145
Dyslipidaemia	22 (73.3%)	37 (68.5%)	0.372
Smoking history			
Current smoker	4 (13.3%)	4 (7.4%)	0.999
Former smoker	5 (16.7%)	12 (22.2%)	0.453
Non-smoker	19 (63.3%)	35(64.8%)	0.754
Family history of CAD	1 (1.9%)	1 (1.9%)	0.453
Angina at presentation			
No chest pain	4 (13.3%)	10 (18.5%)	0.643
Chest pain	9 (30.0%)	20 (37.0%)	0.488
Atypical chest pain	9 (30.0%)	13 (24.1%)	0.582
Nonanginal chest pain	3 (10.0%)	3 (5.6%)	0.590
Fatigue or dyspnoea on exertion	4 (13.3%)	7 (13.0%)	0.999
Positive SPECT findings	15 (50.0%)	22 (40.7%)	0.166
Coronary stenosis > 50% by ICA:			
LAD	11 (36.7%)	17 (31.5%)	0.681
LCX	5 (16.7%)	7 (13.0%)	0.643
RCA	7 (23.3%)	13 (24.1%)	0.955
Coronary stenosis > 70% by ICA:			
LAD	5 (16.7%)	8 (14.8%)	0.810
LCX	5 (16.7%)	7 (13.0%)	0.643
RCA	6 (20.0%)	9 (16.7%)	0.725
Radiation dose in CT (mSv)	6.5 [4.9;7.8]	6.4 [4.7;7.9]	0.671
Total contrast dose (mL)	170.0 [160.0;180.0]	170.0 [167.5;180.0]	0.573

Values are reported as N (%) or median [interquartile range].
Abbreviations: CAD = Coronary artery disease; CT = Computed Tomography; LAD = left anterior descending; LCX = left circumflex artery; RCA = right coronary artery; SPECT = single photon emission computed tomography.

- (c) **Myocardial perfusion reserve index (MPRI)**: the percentage of MA at stress minus MA at rest divided by MA at rest [9].

The quantitative approach which uses short-axis views of the left ventricle as input images was based on an in-house Matlab code (MathWorks, Massachusetts, US) that allowed to: (1) select three anatomical reference points for automatic AHA segmentation, (2) segment the left ventricle wall semi-automatically, (3) define each AHA segment automatically, (4) measure LV myocardial perfusion in each AHA-segment in terms of MA, TPR and MPRI and (5) consider an AHA-segment to be hypoperfused if the corresponding CTP parameter was below one established threshold in this region (Fig. 2). Parameter-specific cut-off values were obtained from the **test group** (Fig. 1). For each parameter, a large range of possible cut-off values were defined and their performances were assessed in terms of Youden index in a vessel-based analysis. The best threshold was defined as the one with the highest Youden Index. Further details on Appendices (A1, A2 and A3).

2.4. Statistical analysis

The Kolmogorov-Smirnov test was used to evaluate distribution normality. Continuous demographic variables were expressed as mean ± standard deviation (SD) if normally distributed and as median [first-third] non-adjusted quartiles otherwise. The Mann-Whitney U test was used with non-normal continuous variables whereas Fisher's exact test or bivariate logistic regression analysis was applied for non-normal categorical variables.

Qualitative and quantitative approaches by single-energy CT or CT-based iodine imaging were compared in terms of accuracy, sensitivity, specificity, positive and negative predictive values (PPV and NPV, respectively), Youden index and the area under the receiver operating characteristic (ROC) curve (AUC). AUC(s) were compared using the approach of DeLong et al. [18]. All data are reported with 95% confidence intervals. Epidat (Xunta de Galicia, Spain; OPS-OMS; Universidad CES, Colombia) was used for the analysis.

3. Results

3.1. Population description

Demographic and clinical characteristics of both **test** and **validation groups** are presented in Table 1. No significant differences were observed in patient characteristics and comorbidities. All patients completed the CTA/CTP protocol with no complications. In the **validation group**, 8 (4.9%) LAD vessels showed significant coronary stenosis (luminal reduction >70%) by ICA and 4 (2.5%) of these were also associated with at least one positive myocardial segment on SPECT. Regarding LCX vessels, 7 (4.3%) showed >70% lumen narrowing by ICA and 5 (3%) of these were related to hypoperfusion by SPECT. Significant stenosis in the RCA was found in 9 cases (5.6%), 8 of which (4.9%) were associated with a perfusion defect by SPECT (Table 1).

3.2. Cut-off values for quantitative perfusion parameters

The cut-off values for perfusion parameters to distinguish normally-perfused from hypoperfused myocardial tissue were determined in a randomly-selected **test group** of 30 patients (Appendices A3). The best-performing thresholds for TPR, MPRI and MA were 0.96, 23 and 0.5 for single-energy CT, and 0.97, 47 and 0.3 for iodine images, respectively.

3.3. Myocardial perfusion analysis from single-energy CT

The diagnostic performance of CTA/CTP compared with SPECT + ICA was assessed in the 54 patients forming the **validation group**. The number of artefacts (motion artefacts, beam hardening, etc) identified through visual interpretation was minimal: only 3% of myocardial segments, which were excluded from the analyses.

3.3.1. Vessel-based analysis

The vessel-based diagnostic performance of CTA/CTP for myocardial perfusion assessment with >70% of lumen narrowing to determine significant coronary stenosis and the use of single-energy CT images is shown in **Table 2**. Visual analysis proved to be an effective and appropriate approach for detecting perfusion defects with high performance in terms of accuracy and AUC.

TPR outperformed the visual method and the other quantitative parameters, thereby providing the highest values of sensitivity, PPV and Youden index (**Table 2**). TPR resulted in the highest AUC [0.99 (0.98–1.00)] compared to that for the visual analysis [0.86 (0.76–0.97); $p = 0.025$ from Delong's test], MPRI [0.95 (0.89–1.01); $p = 0.291$] and MA [0.98 (0.96–1.00); $p = 0.521$]. MPRI showed the lowest sensitivity [94% (79–100)] and AUC [0.95 (0.89–1.01)] among the other quantitative parameters, and TPR provided the highest PPV [81% (62–100)]. Specificity, NPV and accuracy were similar in all cases, although TPR and MA resulted in the highest Youden index and AUC (**Table 2**).

The diagnostic performance of per-vessel CTA/CTP strategy with a lumen narrowing of 50% to define significant coronary stenosis is shown in **Table A2** (Appendices). Similar results than those obtained with the 70% threshold were found: myocardial perfusion assessment was feasible with visual analysis, although quantitative analysis with TPR yielded better results than visual interpretation [AUCs: 0.93 (0.86–0.98) vs. 0.86 (0.77–0.95), respectively; $p = 0.264$]. A case example showing myocardial perfusion assessment with TPR, MA and MPRI is shown in **Fig. 3** (see **Fig. 4**).

3.3.2. Patient-based analysis

The patient-based diagnostic performance of CTA/CTP for myocardial perfusion assessment with 70% coronary stenosis cut-off is shown in **Table 3**. Ischaemia assessment was feasible through visual interpretation of single-energy CT with high specificity, PPV, accuracy and AUC. TPR and MA proved to be the best-performing parameters in terms of sensitivity, Youden index and AUC (**Table 3**). Two false positives were found: one may be a false-negative of SPECT and the other one as a result of the inhomogeneous distribution of contrast. Youden index and AUC of TPR and MA were substantially higher compared to visual analysis and MPRI (**Table 3**).

Table 2

Performance of visual and quantitative myocardial perfusion vessel-based analysis by single- and dual-energy CT.

	Single-energy CT images				CT-based iodine images			
	Visual analysis	TPR	MPRI	MA [HU]	Visual analysis	TPR	MPRI	MA [mg/mL]
<i>Threshold</i>		0.96	23	0.5		0.97	47	0.3
Sensitivity	76 (53–100)	100 (97–100)	94 (79–100)	100 (97–100)	87 (66–100)	100 (97–100)	93 (77–100)	87 (66–100)
Specificity	97 (93–100)	97 (94–100)	97 (93–100)	96 (92–99)	99 (97–100)	94 (89–99)	95 (91–100)	94 (89–99)
PPV	72 (49–96)	81 (62–100)	76 (56–97)	74 (54–94)	93 (76–100)	71 (50–93)	74 (51–96)	68 (45–92)
NPV	97 (94–100)	100 (99–100)	99 (98–100)	100 (99–100)	98 (95–100)	100 (99–100)	99 (97–100)	98 (95–100)
Accuracy	94 (91–98)	98 (95–100)	96 (93–100)	96 (93–100)	97 (94–100)	95 (91–99)	95 (91–99)	93 (88–98)
Youden Index	0.73 (0.53–0.93)	0.97 (0.95–1.00)	0.91 (0.79–1.02)	0.96 (0.93–0.99)	0.86 (0.68–1.03)	0.94 (0.90–0.99)	0.89 (0.75–1.02)	0.81 (0.63–0.99)
AUC on ROC	0.86 (0.76–0.97)	0.99 (0.98–1.00)	0.95 (0.89–1.01)	0.98 (0.96–1.00)	0.93 (0.84–1.02)	0.97 (0.95–0.99)	0.94 (0.87–1.01)	0.90 (0.81–1.00)

Values are % (95% confidence interval).

Abbreviations: AUC = area under the curve; CTA = Computed tomography angiography; CT = Computed tomography; HU = Hounsfield Units; MA = mean attenuation; MPRI = myocardial perfusion reserve index; PPV and NPV = positive and negative predictive values, respectively; ROC = receiver-operating characteristic; TPR = transmural perfusion ratio.

These results were not affected by the choice of the 50% or the 70% coronary stenosis thresholds, the ones with the 50% are shown in **Table A3** (Appendices).

3.4. Myocardial perfusion analysis from dual-energy CT-based iodine imaging

Dual-energy CT was only performed in 40 patients out of the 54 included in the **validation group**.

3.4.1. Vessel-based analysis

The vessel-based diagnostic performance of iodine-based CTA/CTP strategy for myocardial perfusion assessment with a coronary stenosis threshold of 70% is presented in **Table 2**. The AUC obtained with visual analysis of iodine images were higher than those obtained with single-energy CT images [0.93 (0.84–1.02) vs. 0.86 (0.76–0.97); $p = 0.367$].

TPR provided the best performance [AUC: 0.97 (0.95–0.99)] compared with visual method [AUC: 0.93 (0.84–1.02); $p = 0.363$], MA [AUC: 0.90 (0.81–1.00); $p = 0.167$] and MPRI [AUC: 0.94 (0.87–1.01); $p = 0.437$] (**Table 2**). Although specificity and NPV were similar among all approaches; visual method, MPRI and MA resulted in lower sensitivity, Youden index and AUC compared to TPR (**Table 2**).

The 70% or the 50% of lumen narrowing to determine significant coronary stenosis did not affect the CTA/CTP performing results. Visual analysis on CT-based iodine images resulted in higher AUC compared to that on single-energy CT images [0.89 (0.82–0.97) vs. 0.86 (0.77–0.95); $p = 0.564$] for the 50% coronary stenosis threshold. TPR yielded higher Youden index and AUC than visual analysis and the other quantitative parameters (**Table A2** Appendices).

3.4.2. Patient-based analysis

The patient-based diagnostic performance of iodine-based CTA/CTP for myocardial perfusion assessment with 70% of coronary stenosis threshold are shown in **Table 3**. As in per-vessel analysis, TPR resulted to be the best-performing method. MPRI and MA performed the worst in terms of Youden index and AUC.

When a 50% of lumen narrowing was used to define significant coronary stenosis, TPR resulted in higher sensitivity, Youden index and AUC compared to MPRI and MA (**Table A3** Appendices).

4. Discussion

In patients with or without suspicion of CAD, a single CT examination including CTA and CTP has proven to be effective for detect-

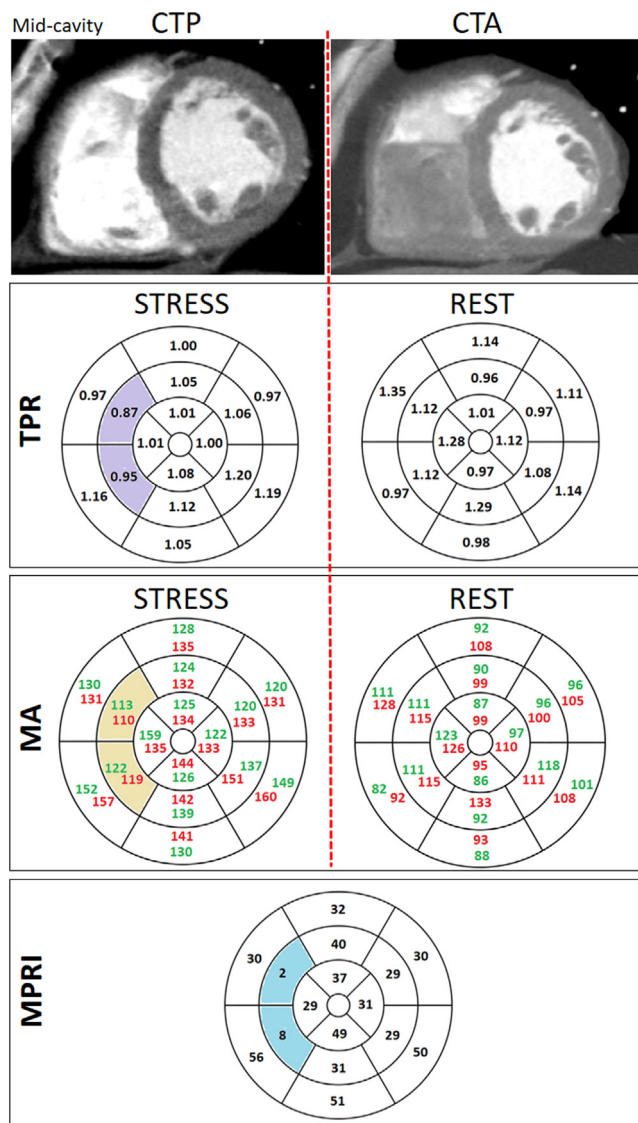


Fig. 3. Case example showing quantitative myocardial perfusion analyses with transmural perfusion ratio (TPR), mean attenuation (MA) and myocardial perfusion reserve index (MPRI) from single-energy CT in a 49-year-old patient with typical chest pain. Static single-energy CT images at the mid-ventricular short-axis view at Dipyridamole-induced stress (CTP) (left) and at rest (CTA) (right). 16-AHA segmentation of the left ventricle wall was performed. (A) TPR was calculated automatically as the ratio of the segment-specific mean attenuation (MA) in the subendocardium to the MA of the entire subepicardial layer at stress (left) and rest (right). (B) MA was quantified at the subendocardium (red values) and the subepicardium (green values) at stress (left) and rest (right). (C) MPRI was computed as the percentage of MA at stress minus MA at rest divided by MA at rest. AHA-segments associated with TPR < 0.96, MA < mean-0.5-standard deviation (of all subendocardial MA values at rest or stress) or MPRI < 26 are shown in purple, yellow and blue, respectively. Significant coronary stenosis (>70% lumen narrowing) in the proximal left anterior descending artery (LAD) was confirmed by CTA. (For interpretation of the references to colour in this figure legend, the reader is referred to the web version of this article.)

ing both coronary stenosis and myocardial hypoperfusion [2]. To the best of authors' knowledge, this is the first study to compare visual interpretation and three previously-proposed perfusion parameters (TPR, MPRI, and MA) [3–5,9] and compare their performance in ischaemia assessment for both single-energy CT and CT-based iodine studies.

The main findings of this study were that: (1) visual interpretation on single-energy CT was effective in detecting myocardial ischaemia compared with SPECT + ICA; (2) visual identification

on dual-energy CT-based iodine images performed better than visual analysis on single-energy CT; and (3) on both CT-imaging modalities TPR was the best-performing method among visual analysis and the other parameters for detecting myocardial ischaemia.

In this study, rest CTA images were acquired before CTP as suggested in several studies such as the CORE320 [2] to facilitate translation to clinical care. Patients with normal or near-normal coronary vessels in CTA images will not generally need perfusion imaging, and patients with intermediate degrees of coronary stenosis would then proceed to having a stress CTP for clinical decision-making. Moreover, if CTA precedes CTP, the assessment of coronary stenosis on CTA should be more accurate and CTA image quality may not be affected by the high cardiac frequency as effect of Dipyridamole.

4.1. Diagnostic performance with single-energy CT

Of note, the conclusions of the present study were not substantially affected by the choice of the 50% or 70% threshold.

Visual analysis of CTA/CTP images for myocardial perfusion assessment in addition to coronary anatomy information by CTA was as useful as SPECT + ICA in CAD diagnosis. Our results in terms of specificity and NPV, which neared 95% for both coronary thresholds (>50% and >70%), are in line with those of two studies based on the CORE320 data. In those works, in which CTA/CTP + coronary CTA (>50%) was compared to SPECT + ICA, specificity values were close to 90% [2,19].

TPR outperformed visual analysis as well as MA and MPRI. This result, which held true for both 50% and 70% stenosis thresholds, supports the use of TPR compared to MA and MPRI for an ischaemia CT-image assessment. The diagnostic performance of TPR (<0.85) + coronary CTA(>70%) was assessed by Cury et al. [5] using SPECT + ICA as the reference method. The results of the present study (Table 2) are in line with those of Cury et al, showing similar sensitivity [94% (71–100)] and PPV [89% (64–99)] in the per-patient analysis. However, they reported lower specificity [78% (40–97)] and AUC [0.85 (0.66–0.96)] compared to those obtained in this work.

Several authors have reported the good performance of TPR on detecting ischaemia [4,5,20]. However, whether quantitative myocardial perfusion assessment is superior to visual analysis is not well established. Some authors found the potential of TPR [4,5,20], whereas others did not find its incremental value [3,6]. Pontone et al. [6] found that the addition of stress-CTP with visual evaluation to coronary CTA imaging had similar diagnostic performance on detecting ischaemia when compared with TPR. These discrepancies may be related to (i) the use of different thresholds for TPR, (ii) different reference methods for validation (fractional flow reserve (FFR), SPECT, SPECT + ICA, CMR, etc.), (iii) differences in the study population and (iv) different thresholds for the definition of significant coronary stenosis.

4.2. Diagnostic performance with CT-based iodine imaging

This study is the first to quantify TPR, MPRI and MA from CT-based iodine images and demonstrate that TPR resulted in higher sensitivity, Youden index and AUC than visual interpretation. It was also observed that visual analysis on iodine images provided better results than the visual interpretation on single-energy CT images.

Myocardial ischaemia based on visual interpretation of iodine distribution has not been extensively studied. Ko et al. [21] demonstrated the incremental diagnostic value of combined coronary CTA and iodine CTP compared to coronary CTA alone for the detection of significant coronary stenosis. Compared to present results, sim-

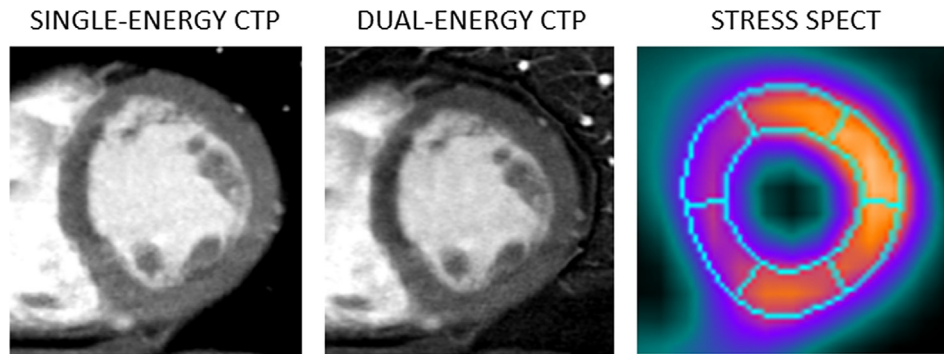


Fig. 4. Stress single-energy (first column) and dual-energy (second column) CT perfusion (CTP), and SPECT (third column) for a 49-year-old patient without prior history of coronary artery disease and with chest pain symptoms. Both single- and dual-energy CTP studies as well as SPECT at the mid-ventricular short-axis view revealed ischemia in the mid anteroseptal and inferoseptal segments.

Table 3
Performance of visual and quantitative myocardial perfusion patient-based analysis by single- and dual-energy CT.

	Single-energy CT images				CT-based iodine images			
	Visual analysis	TPR	MPRI	MA [HU]	Visual analysis	TPR	MPRI	MA [mg/mL]
Threshold		0.96	23	0.5		0.97	47	0.3
Sensitivity	90 (66–100)	100 (95–100)	90 (66–100)	100 (95–100)	88 (58–100)	100 (94–100)	89 (63–100)	89 (63–100)
Specificity	95 (88–100)	95 (88–100)	93 (85–100)	95 (88–100)	100 (98–100)	94 (83–100)	94 (83–100)	94 (83–100)
PPV	82 (54–100)	83 (58–100)	75 (46–100)	83 (58–100)	100 (93–100)	82 (54–100)	80 (50–100)	80 (50–100)
NPV	98 (92–100)	100 (99–100)	98 (92–100)	100 (99–100)	97 (90–100)	100 (98–100)	97 (89–100)	97 (89–100)
Accuracy	94 (87–100)	96 (90–100)	93 (85–100)	96 (90–100)	98 (91–100)	95 (87–100)	93 (83–100)	93 (83–100)
Youden Index	0.85 (0.66–1.05)	0.95 (0.89–1.02)	0.83 (0.64–1.03)	0.95 (0.89–1.02)	0.88 (0.65–1.10)	0.94 (0.85–1.02)	0.82 (0.60–1.05)	0.82 (0.60–1.05)
AUC on ROC	0.93 (0.82–1.03)	0.98 (0.95–1.00)	0.92 (0.81–1.02)	0.98 (0.95–1.01)	0.94 (0.81–1.06)	0.97 (0.92–1.01)	0.92 (0.79–1.03)	0.92 (0.79–1.03)

Values are % (95% CI).

Abbreviations: AUC = area under the curve; CI = confidence interval; CTA = Computed tomography angiography; CT = Computed tomography; HU = Hounsfield Units; MA = mean attenuation; MPRI = myocardial perfusion reserve index; PPV and NPV = positive and negative predictive values, respectively; ROC = receiver-operating characteristic; TPR = transmural perfusion ratio.

ilar sensitivity [88% (81–93)] and NPV [91% (86–95)] but lower specificity [79% (73–85%)], PPV [73% (65–80)] and AUC [0.84 (0.79–0.88)] were obtained.

Our analyses revealed that the use of iodine as a perfusion measure led to a reduction in the number of artefacts, better image quality, fewer false-negatives and a higher detection rate of perfusion defects which might be misdiagnosed by SPECT + ICA.

4.3. Study limitations

First, ICA + FFR would have been the best reference method. Nonetheless, SPECT + ICA was used here because the study population had already had a SPECT to detect ischemia and to avoid coronary manipulation with wires in non-significant coronary stenosis. Second, the use of a 64-slice CT scanner may lead to a greater number of artefacts compared to those obtained with more advanced CT systems. However, the ASiR technology used here to reconstruct CT images has proven to result in noise reduction and significantly impacted image quality, thereby improving the proportion of interpretable myocardial segments compared with filtered backprojection (FBP) reconstruction [14]. Furthermore, several studies have proven the potential application of 64-slice CT scanners in the detection of myocardial ischaemia [7,17,22] and the number of artefacts identified through visual interpretation in this study was minimal: only 3% of myocardial segments were excluded for the analysis. Third, myocardial segments were associated with one of the three major coronary arteries based on the established clinical recommendations. Nonetheless, the variability in coronary circulation may result in different coupling between coronary arteries and LV segments. Fourth, a total of 33 (3.8%) myocardial segments had ischaemia by SPECT without significant coronary

stenosis (lumen narrowing >50%). Thirteen and 19 of them (1.5% and 2.9%, respectively) were also identified as ischaemic segments by visual analysis on single-energy CT and iodine CT-based images, respectively. The hypoperfused segments detected by SPECT and not by CT or vice versa without significant coronary stenosis may be false-positive or false-negative results of one of these techniques. Conversely, ischaemic myocardial segments identified by both SPECT and CT without significant coronary stenosis may be due to microvascular ischaemia. This last statement may be investigated with the use of another technique for detecting myocardial ischemia, such as magnetic resonance imaging, which is not available in this study.

Finally, performance of both visual and quantitative analyses may appear unusually high. In this study, consecutive patients were referred for an ICA after SPECT based on the following clinical criteria in order to minimize patient risk and reduce invasive procedures: positive SPECT (37 patients with ischemia) or persistent symptomatology with negative SPECT (47 patients). The fact of excluding patients with known CAD or prior revascularization (without stent or by-pass) implies lower probability of having significant CAD in the population and probably better results in analyses of myocardial ischaemia. Maybe the high threshold of lumen narrowing (>70%) to determine significant coronary stenosis and the use of advanced ASiR reconstruction technique may have contribute to these results.

5. Conclusions

CT myocardial perfusion analysis by visual interpretation proved to be effective in detecting myocardial ischaemia compared to SPECT + ICA, although the use of quantitative data in terms of

TPR improves its detection. However, visual interpretation of myocardial perfusion on dual-energy CT-based iodine images outperforms visual analysis on single-energy CT, thereby being less necessary the use of quantitative methods in this case.

Declaration of Competing Interest

The authors declare that they have no known competing financial interests or personal relationships that could have appeared to influence the work reported in this paper.

Appendix A

A1. AHA segmentation of the left ventricle

The left ventricle on CTA and CTP was divided into equal thirds perpendicular to the long axis based on anatomical landmarks and following the published recommendations [15]. The basal third was acquired and displayed from the area extending from the mitral annulus to the tips of the papillary muscles, the mid-cavity view was selected from the region that includes the entire length of the papillary muscles, and the apical short-axis view was selected from the area beyond the papillary muscles to just before the cavity ends. The slice thickness was of 0.8 cm and determined on the basis of modality-specific resolution.

AHA-segmentation of the left ventricle was performed using three short-axis views of the left ventricle (basal, mid and apical sections) both at rest and under stress by an experienced observer.

As suggested, for each of the six short-axis views (3 at rest and 3 at stress), three reference points were selected (Fig. A1, top): the first one situated on the external contour of the ventricle wall that separates the anterior and the anteroseptal (or septal, in the case of apical section) segments, the second one located on the center of the lumen and the third one situated on the external contour of the ventricle wall that separates the inferior and the inferoseptal (or septal) segments.

The left ventricle wall segmentation was done by Region Growing, an algorithm which allows the partitioning of an image into similar/homogenous areas through the application of homogeneity/similarity criteria such as colour, intensity and/or texture, by in-house Matlab code (MathWorks, Massachusetts, US). The mask and reference points were transformed from Cartesian into Polar Coordinate System and the angles of reference points were used to extract myocardial AHA segments automatically (Fig. A1, bottom).

A2. Evaluation of myocardial perfusion defects according to quantitative CTP parameters: MA, TPR, and MPRI

Mean attenuation density (MA)

For both rest- and stress CT images, mean attenuation values of the 16 AHA-segments were calculated at subendocardium, subepicardium and whole-myocardium providing six mean and standard deviation (SD) values of attenuation (3 at rest and 3 at stress). The subendocardium, the subepicardium and whole-myocardium of each AHA- segment which presented an attenuation value lower than the mean-kSD, were classified as hypoperfused. Different

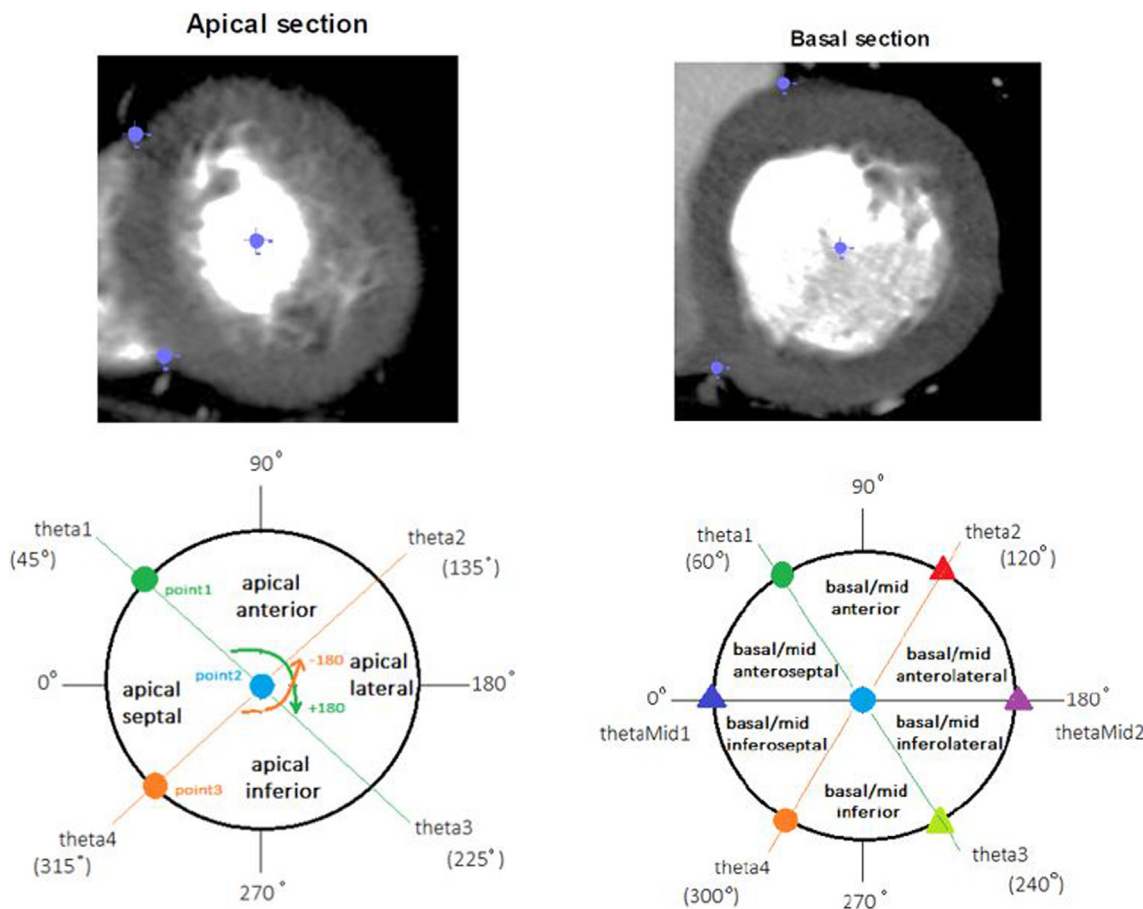


Fig. A1. AHA segmentation of the apical (left) and basal (right) sections in a theoretically case in which the angles of the reference points 1, 2 and 3 were 45, 0 and 315 degrees, respectively, for the apical section; and 60, 0 and 300 degrees for the basal section.

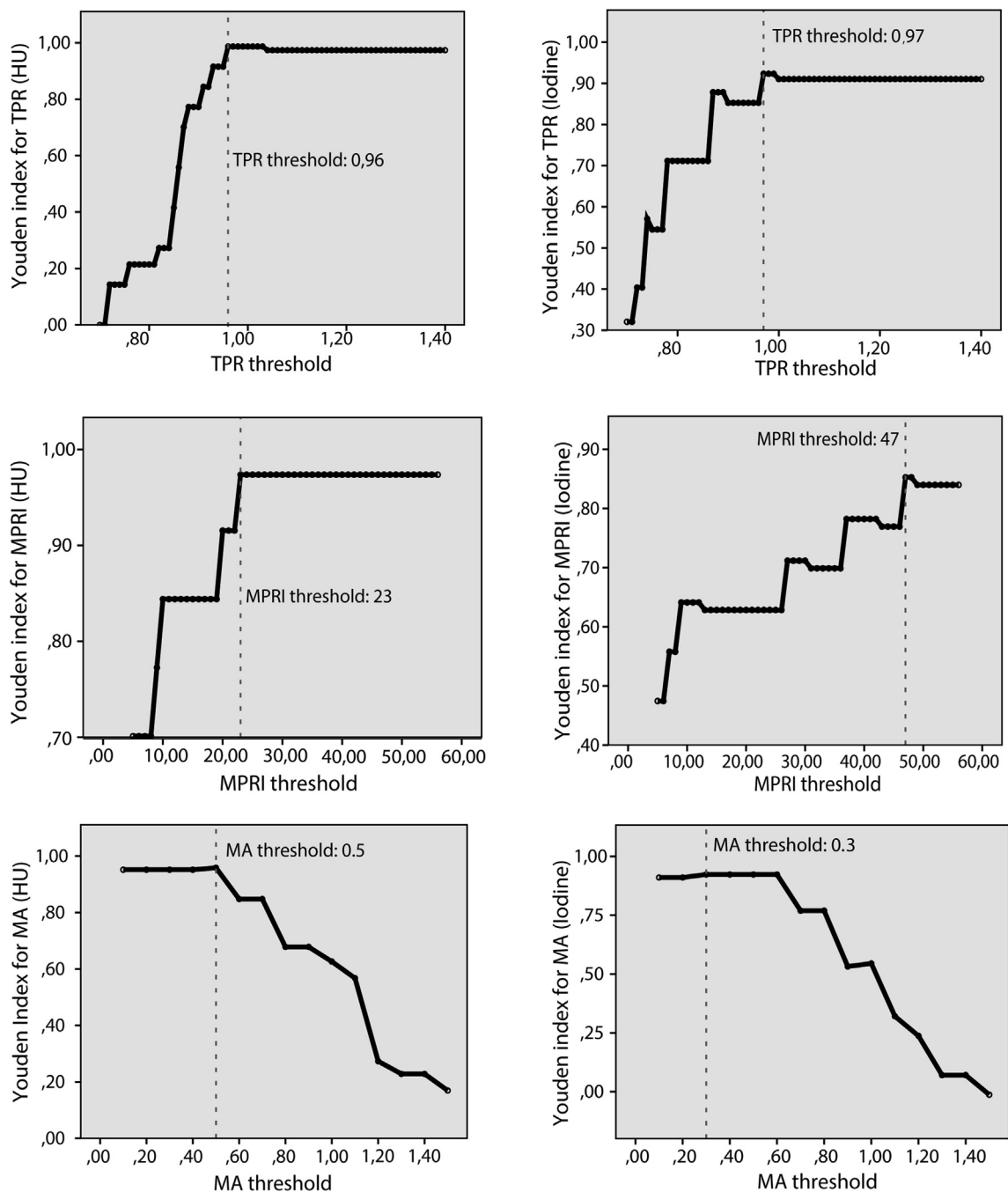


Fig. A2. Cut-off values determination for myocardial perfusion computed topography (CT) parameters. Youden index versus different thresholds for transmural perfusion ratio (TRP) (first row), myocardial perfusion reserve index (MPRI) (second row) and mean attenuation (MA) (third row) by conventional CT (left column) and CT-based iodine imaging (right column).

thresholds (k) were analyzed (Fig. A2). Perfusion defects were identified as the AHA-segments with hypoperfusion in at least the subendocardium or in the whole myocardium at stress (ischemia) or at both rest and stress (infarction). Those segments with an MA value below the threshold at the subepicardium but not at subendocardium were categorized as artifacts.

Transmural perfusion ratio (TPR)

Two TPR values from both rest and stress images were obtained per segment. Hypoperfusion was defined if TPR value was below the threshold in the stress-phase (ischemia) or in both rest- and stress-phases (infarct).

Myocardial perfusion reserve index (MPRI)

An MPRI value was obtained per each segment, so hypoperfusion was defined if that value was below the threshold.

A3. Cut-off values of CTP parameters

Single-energy CT and CT-based iodine imaging are quantified using different measuring units, Hounsfield Units and mg/mL of iodine, respectively; for this reason, two sets of thresholds were determined. For both native and iodine imaging, the 90 main coronary vessels (LAD, LCX or RCA) of the test group (30 patients, randomly-selected among those having both images available)

Table A1
Cut-off parameter determination in the test group. Performance results of quantitative vessel-based perfusion analysis with coronary CTA > 70%.

	Single-energy CT images			CT-based iodine images		
	TPR	MPRI	MA	TPR	MPRI	MA
<i>Threshold</i>	0.96	23	0.5	0.97	47	0.3
Sensitivity	100 (96–100)	100 (96–100)	100 (94–100)	100 (96–100)	92 (72–100)	100 (96–100)
Specificity	99 (95–100)	97 (93–100)	97 (93–100)	92 (86–99)	94 (87–100)	92 (86–99)
PPV	93 (77–100)	87 (68–100)	87 (68–100)	67 (42–91)	69 (43–95)	67 (42–91)
NPV	100 (99–100)	100 (99–100)	100 (99–100)	100 (99–100)	99 (95–100)	100 (99–100)
Accuracy	99 (96–100)	98 (94–100)	98 (94–100)	93 (88–99)	93 (88–99)	93 (88–99)
Youden Index	0.99 (0.96–1.01)	0.97 (0.94–1.01)	0.97 (0.94–1.01)	0.92 (0.86–0.98)	0.85 (0.69–1.02)	0.92 (0.86–0.98)
AUC on ROC	0.99 (0.98–1.00)	0.98 (0.97–1.01)	0.98 (0.97–1.01)	0.96 (0.93–0.99)	0.93 (0.84–1.01)	0.96 (0.93–0.99)

Values are % (95% CI).

Abbreviations: AUC = area under the curve; CI = confidence interval; CTA = Computed tomography angiography; CT = Computed tomography; MA = mean attenuation; MPRI = myocardial perfusion reserve index; PPV and NPV = positive and negative predictive values, respectively; ROC = receiver-operating characteristic; TPR = transmural perfusion ratio.

Table A2
Per-vessel CT myocardial perfusion analysis with validation group. Performance results of visual and quantitative perfusion analysis with single-energy CT or dual-energy CT-based iodine images and coronary CTA > 50%.

	Single-energy CT images			CT-based iodine images				
	Visual analysis	TPR	MPRI	MA	Visual analysis	TPR	MPRI	MA
<i>Threshold</i>		0.96	23	0.5		0.97	47	0.3
Sensitivity	75 (56–94)	92 (79–100)	92 (79–100)	96 (86–100)	82 (66–100)	95 (84–100)	86 (70–100)	82 (63–100)
Specificity	97 (94–100)	93 (88–97)	92 (87–97)	91 (86–96)	96 (91–100)	89 (82–96)	91 (85–97)	89 (82–96)
PPV	82 (63–100)	69 (51–86)	67 (49–84)	66 (49–83)	82 (66–100)	66 (48–84)	68 (49–87)	62 (43–81)
NPV	96 (92–99)	98 (96–100)	98 (96–100)	99 (97–100)	96 (91–100)	99 (96–100)	97 (93–100)	96 (91–100)
Accuracy	92 (90–98)	93 (88–97)	92 (87–96)	92 (87–96)	93 (88–98)	90 (84–96)	90 (84–96)	87 (81–94)
Youden Index	0.72 (0.55–0.90)	0.86 (0.73–0.96)	0.82 (0.72–0.96)	0.87 (0.78–0.96)	0.81 (0.65–0.96)	0.84 (0.74–0.95)	0.77 (0.62–0.93)	0.71 (0.53–0.88)
AUC on ROC	0.86 (0.77–0.95)	0.93 (0.86–0.98)	0.90 (0.86–0.98)	0.90 (0.89–0.98)	0.89 (0.82–0.97)	0.92 (0.87–0.98)	0.89 (0.81–0.96)	0.85 (0.76–0.94)

Values are % (95% CI).

Abbreviations: AUC = area under the curve; CI = confidence interval; CTA = Computed tomography angiography; CT = Computed tomography; MA = mean attenuation; MPRI = myocardial perfusion reserve index; PPV and NPV = positive and negative predictive values, respectively; ROC = receiver-operating characteristic; TPR = transmural perfusion ratio.

Table A3
Per-patient CT myocardial perfusion analysis with validation group. Performance results of visual and quantitative perfusion analysis with single-energy CT or dual-energy CT-based iodine images and coronary CTA > 50%.

	Single-energy CT images			CT-based iodine images				
	Visual analysis	TPR	MPRI	MA	Visual analysis	TPR	MPRI	MA
<i>Threshold</i>		0.96	23	0.5		0.97	47	0.3
Sensitivity	87 (66–100)	93 (77–100)	93 (77–100)	100 (97–100)	93 (75–100)	100 (96–100)	86 (64–100)	93 (76–100)
Specificity	95 (86–100)	89 (78–100)	85 (72–97)	85 (72–97)	95 (79–100)	81 (64–98)	81 (64–98)	81 (64–98)
PPV	87 (66–100)	78 (56–100)	70 (47–93)	71 (50–93)	87 (66–100)	74 (51–96)	71 (46–95)	72 (49–96)
NPV	95 (86–100)	97 (90–100)	97 (90–100)	100 (98–100)	96 (85–100)	100 (98–100)	91 (78–100)	95 (84–100)
Accuracy	93 (84–100)	91 (82–99)	87 (77–97)	89 (80–98)	92 (78–100)	87 (76–99)	82 (69–96)	85 (73–97)
Youden Index	0.81 (0.63–1.00)	0.84 (0.67–0.99)	0.78 (0.61–0.95)	0.85 (0.73–0.96)	0.85 (0.67–1.02)	0.81 (0.66–0.96)	0.66 (0.43–0.90)	0.74 (0.53–0.94)
AUC on ROC	0.90 (0.81–1.00)	0.92 (0.83–1.00)	0.89 (0.80–0.98)	0.92 (0.87–0.98)	0.92 (0.83–1.01)	0.90 (0.83–0.98)	0.83 (0.71–0.95)	0.87 (0.76–0.97)

Values are % (95% CI).

Abbreviations: AUC = area under the curve; CI = confidence interval; CTA = Computed tomography angiography; CT = Computed tomography; MA = mean attenuation; MPRI = myocardial perfusion reserve index; PPV and NPV = positive and negative predictive values, respectively; ROC = receiver-operating characteristic; TPR = transmural perfusion ratio.

were classified as having coronary artery disease if they had both a lumen narrowing >70% by invasive coronary angiography (ICA) and at least one myocardial segment of the myocardial territory ascribed to the narrowed coronary artery with a specific myocardial perfusion CT parameter < threshold. For each parameter a large range of possible cut-off values were defined taking into account that minimum and maximum analyzed thresholds were bounded by taking into account lowering both false negatives with too high cut-off values and false positives with too low thresholds. The performance of each threshold on both single-energy CT and

iodine imaging were compared with SPECT + ICA as reference in terms of Youden index (Fig. A2). Finally, the best thresholds were determined as those with the highest Youden Index (Table A1).

In the case of HU, the best-performing results of TPR, MPRI, and MA were raised with 0.96, 23 and 0.5, respectively, in accordance with Youden indexes of 0.99 for TPR and 0.97 for both MPRI and MA (Table A1). In the case of iodine, the best cut-off values for TPR, MPRI and MA were 0.97, 47 and 0.3, respectively, with Youden indexes of 0.96 for both TPR and MA, and 0.93 for MPRI (Table A1).

Table A4
Overview of dissenting CTA/CTP results compared to the reference method (SPECT + ICA) and reasons for those errors in 4 cases: visual analysis and TPR with the use of single-energy CT or iodine images.

Patient ID	Vessel	Type of false result on CT	Reason for false results on CT			
			Single-energy CT images		CT-based iodine images	
			Visual analysis	TPR	Visual analysis	TPR
A	LAD	FP	Artifact	Artifact	FN of SPECT	FN of SPECT
B	LAD	FP	Contrast distribution	Contrast distribution		Contrast distribution
	LCX	FP		Artifact		FN of SPECT
C	LAD	FP	FN of SPECT	FN of SPECT		FN of SPECT
	RCA	FP	FN of SPECT			FN of SPECT
D	LAD	FP	Contrast distribution			Contrast distribution
E	RCA	FN	Image quality		Impossible to detect visually	
F	LAD	FN	Image quality		Impossible to detect	
	LCX	FN	Image quality			
	RCA	FN	Image quality			
G	RCA	FN				
	LCX	FN				

Abbreviations: ID = arbitrary identification; LAD = left anterior descending; LCX = left circumflex artery; RCA = right coronary artery; TPR = transmural perfusion ratio; FN = false negative; FP = false positive; SPECT = single-photon emission computed tomography.

A4. Dissenting CTA/CTP results when compared to reference SPECT + ICA in myocardial perfusion analysis

As diagnostic inaccuracies between CTA/CTP and SPECT + ICA occurred in only seven patients, those with dissenting results are referred to as patients A to G in the following sections (Table A4).

Myocardial perfusion analysis from single-energy CT

Visual assessment in the vessel-based analysis resulted in 5 false-positive and 4 false-negative vessels. The majority of false-positive results appeared in the LAD artery due to beam-hardening streaking artefacts (patient A) or to the inhomogeneous distribution of contrast (patients B and D). On the other hand, CT images of patient C, who presented coronary stenosis > 70% in the RCA and LAD, showed subendocardial hypoperfusion along the basal- anteroseptal, inferoseptal and inferior segments which was not identified by SPECT. The correct association between these coronary stenoses and hypoperfused regions might be related to perfusion deficits undetected by SPECT. The 4 false-negative results were found in patients E and F owing to the limited quality of the images (Table A4 Appendices). Three patients were misdiagnosed: two false positives (patients B and C) and one false negative (patient F) (Table A4 Appendices).

No false-negative vessels were detected with TPR although a total of 4 false-positive vessels were identified in three patients (patient A: 1 in LAD, patient B: 1 in LAD and 1 in LCX, patient C: 1 in LAD).

Myocardial perfusion analysis from dual-energy CT-based iodine imaging

Visual iodine-based analysis yielded a false-positive vessel in the LAD of patient A, which may be a perfusion defect undetected by SPECT, as stated previously. On the other hand, 2 false-negative vessels were detected: one in the RCA of patient D, in whom a small subendocardial perfusion defect in the apical inferior segment was detected with TPR but not by visual interpretation, and the other in the LAD of patient E (Table A4 Appendices).

Using TPR, only patient B had a false positive whereas, using the visual approach, only patient D had a false negative.

References

[1] V.L. Roger, A.S. Go, D.M. Lloyd-Jones, et al., Heart disease and stroke statistics-2011 update: a report from the American Heart Association, *Circulation* 123 (2011), <https://doi.org/10.1161/CIR.0b013e3182009701>.
 [2] C.E. Rochitte, R.T. George, M.Y. Chen, et al., Computed tomography angiography and perfusion to assess coronary artery stenosis causing

perfusion defects by single photon emission computed tomography: the CORE320 study, *Eur. Heart J.* 35 (2014) 1120–1130, <https://doi.org/10.1093/eurheartj/eh488>.
 [3] B.S. Ko, J.D. Cameron, M. Leung, et al., Combined CT coronary angiography and stress myocardial perfusion imaging for hemodynamically significant stenoses in patients with suspected coronary artery disease: a comparison with fractional flow reserve, *JACC Cardiovasc. Imag.* 5 (2012) 1097–1111, <https://doi.org/10.1016/j.jcmg.2012.09.004>.
 [4] R.T. George, A. Arbab-Zadeh, J.M. Miller, et al., Adenosine stress 64-and 256-row detector computed tomography angiography and perfusion imaging: a pilot study evaluating the transmural extent of perfusion abnormalities to predict atherosclerosis causing myocardial ischemia, *Circ. Cardiovasc. Imag.* 2 (2009) 174–182, <https://doi.org/10.1161/CIRCIMAGING.108.813766>.
 [5] R.C. Cury, T.A. Magalhaes, A.T. Paladino, et al., Dipyridamol stress and rest transmural myocardial perfusion ratio evaluation by 64 detector-row computed tomography, *J. Cardiovasc. Comput. Tomog.* 5 (2011) 443–448.
 [6] G. Pontone, D. Andreini, A.I. Guaricci, et al., Quantitative vs. qualitative evaluation of static stress computed tomography perfusion to detect haemodynamically significant coronary artery disease, *Eur. Heart J. Cardiovasc. Imag.* 19 (2018) 1244–1252, <https://doi.org/10.1093/ehjci/jey111>.
 [7] K. Hosokawa, A. Kurata, T. Kido, et al., Transmural perfusion gradient in adenosine triphosphate stress myocardial perfusion computed tomography, *Circulat. J.* 75 (2011) 1905–1912, <https://doi.org/10.1253/circj.CJ-10-1144>.
 [8] B.S. Ko, J.J. Linde, A.R. Ihdahid, et al., Non-invasive CT-derived fractional flow reserve and static rest and stress CT myocardial perfusion imaging for detection of haemodynamically significant coronary stenosis, *Int. J. Cardiovasc. Imag.* 35 (2019) 2103–2112, <https://doi.org/10.1007/s10554-019-01658-x>.
 [9] J.T. Kühl, R.T. George, V.C. Mehra, et al., Endocardial-epicardial distribution of myocardial perfusion reserve assessed by multidetector computed tomography in symptomatic patients without significant coronary artery disease: insights from the CORE320 multicentre study, *Eur. Hear J. - Cardiovasc. Imag.* 9 (2015), <https://doi.org/10.1093/ehjci/jev206>.
 [10] A. So, J. Hsieh, S. Narayanan, et al., Dual-energy CT and its potential use for quantitative myocardial CT perfusion, *J. Comput. Tomog.* 6 (2012) 308–317, <https://doi.org/10.1016/j.jcct.2012.07.002>.
 [11] F.J. Klocke, M.G. Baird, B.H. Lorell, et al., ACC/AHA guideline ACC/AHA/ASNC guidelines for the clinical use of cardiac radionuclide imaging – executive summary, *J. Am. College Cardiol.* 42 (2003) 1318–1333, [https://doi.org/10.1016/S0735-1097\(03\)01090-8](https://doi.org/10.1016/S0735-1097(03)01090-8).
 [12] P. Lancellotti, J.L. Zamorano, G. Habib, L. Badano, *The EACVI Textbook of Echocardiography*, 2nd ed., Oxford University Press, Oxford, UK, 2017.
 [13] T.A. Fuchs, J. Stehli, M. Fiechter, et al., First experience with monochromatic coronary computed tomography angiography from a 64-slice CT scanner with Gemstone Spectral Imaging (GSI), *J. Cardiovasc. Comput. Tomog.* 7 (2013) 25–31, <https://doi.org/10.1016/j.jcct.2013.01.004>.
 [14] J. Leipsic, T.M. Labounty, B. Heilbron, et al., Adaptive Statistical Iterative Reconstruction: Assessment of Image Noise and Image Quality in Coronary CT Angiography, 2010, pp. 649–654, <https://doi.org/10.2214/AJR.10.4285>.
 [15] M.D. Cerqueira, N.J. Weissman, V. Dilsizian, A.K. Jacobs, S. Kaul, W.K. Laskey, D. J. Pennell, J.A. Rumberger, T. Ryan, M.S. Verani, Standardized myocardial segmentation and nomenclature for tomographic imaging of the heart: a statement for healthcare professionals from the cardiac imaging committee of the council on clinical cardiology of the American heart association, *Circulation* 105 (2002) 539–542, <https://doi.org/10.1067/mje.2002.123374>.
 [16] G.L. Raff, Abidov A Chair, et al., SCCT guidelines for the interpretation and reporting of coronary computed tomographic angiography, *J. Cardiovasc. Comput. Tomog.* 3 (2009) 122–136, <https://doi.org/10.1016/j.jcct.2009.01.001>.
 [17] E.D. Nicol, J. Stirrup, E. Reyes, et al., Sixty-four-slice computed tomography coronary angiography compared with myocardial perfusion scintigraphy for

- the diagnosis of functionally significant coronary stenoses in patients with a low to intermediate likelihood of coronary artery disease, *J. Nucl. Cardiol.* 15 (2008) 311–318, <https://doi.org/10.1016/j.nuclcard.2008.02.017>.
- [18] E.R. DeLong, D.M. DeLong, D.L. Clarke-Pearson, Comparing the areas under two or more correlated receiver operating characteristic curves: a nonparametric approach, *Biometrics* 44 (1998) 837–845, <https://doi.org/10.3847/0067-0049/227/2/20>.
- [19] T.A. Magalhaes, S. Kishi, R.T. George, et al., Combining coronary angiography and myocardial perfusion by computed tomography in the identification of flow-limiting stenosis – the CORE320 study: a coronary CTA/myocardial CTP integrated analysis, *Am. J. Cardiol.* 116 (2016) 379–383, <https://doi.org/10.1016/j.amjcard.2015.04.051.Predictors>.
- [20] J.J. Linde, J.T. Kühl, J.D. Hove, et al., Transmural myocardial perfusion gradients in relation to coronary artery stenoses severity assessed by cardiac multidetector computed tomography, *Int. J. Cardiovasc. Imag.* 31 (2014) 171–180, <https://doi.org/10.1007/s10554-014-0530-9>.
- [21] S.M. Ko, M.G. Song, H.K. Chee, et al., Diagnostic performance of dual-energy CT stress myocardial perfusion imaging: direct comparison with cardiovascular MRI, *Am. J. Roentgenol.* 203 (2014) W605–W613, <https://doi.org/10.2214/AJR.14.12644>.
- [22] G.M. Feuchtnner, F. Plank, C. Pena, et al., Evaluation of myocardial CT perfusion in patients presenting with acute chest pain to the emergency department: comparison with SPECT-myocardial perfusion imaging, *Heart* 98 (2012) 1510–1517, <https://doi.org/10.1136/heartjnl-2012-302531>.